Topological theory of hadrons. II. Baryons

Henry P. Stapp
Lawrence Berkeley Laboratory, University of California, Berkeley, California 94720
(Received 22 October 1982)

The first paper of this series described a method for incorporating spin into the meson sector of the topological theory of hadrons. This second paper extends the theory to all hadrons. It also incorporates into the covariant S-matrix topological framework the group-theoretic properties of the constituent-quark model.

I. EARLY ATTEMPTS

The early attempts[1-6] to include baryons in the topological expansion corresponded to picturing the baryon as a set of three surfaces arranged like the feathers of an arrow, with each outer edge a quark line and all three inner edges placed in close proximity to a single "dotted' line called by various authors a dotted, junction, or mating line. Within the context of the topological expansion this picture arose in several ways, first as the basis of a simple solution to the purely topological problem of extending the meson topological expansion scheme to three-quark baryons,[1] then from ideas based on QCD (Refs. 2 and 3), and finally from attempts to extend to baryons the idea of the ordered S matrix.[4,5] These different approaches all led to essentially the same conclusion regarding the nature of surfaces of zero complexity, or zero entropy: the zero-entropy surfaces were those that could be generated from a disk by a finite number of operations, each of which consists of attaching two *new* disks to some linear portion of the boundary of the surface obtained from the preceding operations, as indicated in Fig. 1. The surfaces that can be constructed by this procedure are called elementary surfaces.[6]

One defect of this identification of zero-entropy surfaces with elementary surfaces arises from the fact that an elementary surface is separated by a cut into two elementary surfaces if and only if the cut is a tree graph.[6] Thus if a non-tree-graph cut separates an elementary surface into two connected parts, then these two parts are not both elementary (see Fig. 2). Non-tree-graph cuts disrupt, therefore, the entropy property that parts are never more complex than the whole, and prevent an orderly topological expansion in which the zero-entropy level is closed in the sense that the discontinuities of zero-entropy functions depend only on zero-entropy functions.

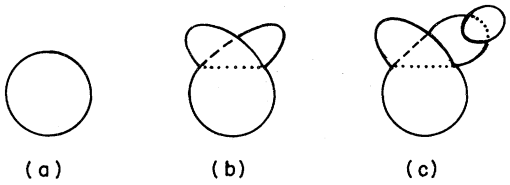

FIG. 1. Three elementary surfaces.

The ordered S-matrix approach leads to rules[3,4] on the ways two zero-entropy surfaces can be joined together to give contributions to zero-entropy amplitudes. These rules are, however, not invariant under the operations of crossing and cluster decomposition, and consequently the singularities associated with a given fixed Landau diagram can be classified as zero entropy in some channels but nonzero entropy in other channels. Hence a single singularity surface can belong to different terms in the topological expansion in different channels. An example is shown in Fig. 3. According to the ordered S-matrix rules the diagram of Fig. 3(a) contributes to the zero-entropy function whereas that of Fig. 3(b) does not. But channel-dependent classifications of this kind lead to unacceptable complications in the analytic structure of the zero-entropy functions, such as the intrusion into their physical sheets of singularities that in the physical functions are buried on unphysical sheets, or are not present at all.

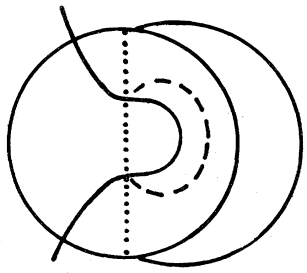

FIG. 2. An elementary surface separated into two parts by a non-tree-graph cut.

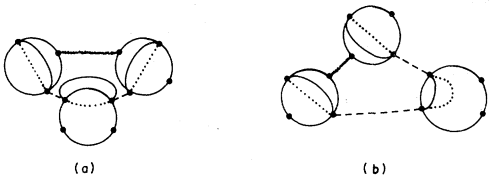

FIG. 3. The graphs that represent in different channels the discontinuity around a single triangle-diagram singularity surface.

A further difficulty with all these approaches is that zero-entropy amplitudes contain singularities corresponding to nonplanar Landau diagrams, and hence presumably have cuts in the complex angular momentum plane.

II. THE ZERO-ENTROPY AMPLITUDES

The difficulties mentioned above can be avoided by treating the three quark lines associated with the baryon unsymmetrically at the zero-entropy level. This allows one to impose at this level a planar structure similar to that obtained in the meson sector, and to represent a typical baryon ortho-amplitude by any one of the three equivalent graphs shown in Fig. 4.

Figure 4(a) is the quark graph G. Its edges are directed line segments called quark lines. The small arrow next to each quark-line edge j indicates that the edge should be replaced by the ortho-propagator $(p_{aj}\cdot\sigma)/m_{aj}$ in the construction of the zero-entropy amplitude Z^G. For a para-propagator case this small arrow would point in the direction opposite to the direction of the quark line, and would indicate

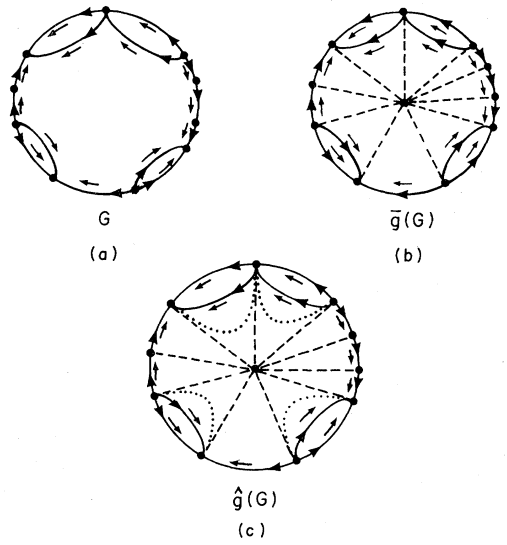

FIG. 4. Three equivalent graphs associated with a typical hadronic amplitude.

that the para-propagator $(-p_{bj}\cdot\sigma)/m_{bj}$ should be used.

Figure 4(b) is the particle-quark graph $\bar{g}(G)$. The dashed-line edges of $\bar{g}(G)$ correspond to particles, and the graph $g(G)$ consisting of the dashed-line edges of $\bar{g}(G)$ and the vertices upon which they begin and end is a Landau graph.

A vertex i of G corresponds to a meson, baryon or antibaryon, or baryonium according to whether two, three, or four quark-line edges are incident upon it. A vertex i with three quark lines terminating on it is called a baryon vertex, and a vertex i with three quark lines originating on it is called an antibaryon vertex.

Except in the trivial two-vertex case each vertex of a quark graph G is connected by edges to exactly two other vertices, which are called its neighbors, and at most two edges connect any pair of vertices. If exactly one quark edge connects two vertices, then this edge is called a solitary quark line. If exactly two quark edges connect a pair of vertices, then these two edges are called paired quark lines.

The diagrams in Figs. 4(a) and 4(b) are planar graphs. But they can also be considered to represent disks bounded by the peripheral quarks lines. Figure 4(c) is a graph $\hat{g}(G)$ that can be considered to represent a surface that is bounded by all the quark lines, and has three sheets joined together at each dotted (i.e., junction) line. The ortho-graph or para-graph character can then be represented by giving each section of the surface (bounded by quark, particle, or junction lines) an orientation that induces on the quark-line boundary a direction that either agrees in the ortho-graph case or disagrees in the para-graph case with the direction of the quark line itself. This surface representation associated with $\hat{g}(G)$ relates the present scheme to the ones proposed earlier. It is used by Chew and Poénaru, who, however, delete from it a small neighborhood of each quark-line vertex. This gives a "feathered" surface analogous to the one bounded by the open diagram D of Fig. 1 of paper I.

The function $Z^G(A)$ associated with G depends on a set of variables A. This set A contains for each vertex i of G a mathematical momentum-energy four-vector p_i. It also contains for each leading end of each quark line j of G a quark variable (α_j,λ_j), and for each trailing end an antiquark variable (β_j,ρ_j). The α_j and β_j are lower undotted and dotted two-valued spinor indices, and λ_j and ρ_j are flavor labels. If the particle associated with vertex i is a Regge recurrence corresponding to orbital angular momentum L_i, then this vertex i is associated with a set of $L_i=L$ pairs of indices

$$(\mu_{il},\sigma_{il},\mu_{i2},\sigma_{i2};\ldots;\mu_{iL},\sigma_{iL}),$$

where μ_{ik} is a vector index associated with orbital angular momentum and σ_{ik} is an associated σ index that will be discussed later.

The function $Z^G(A)$ corresponding to an orthograph G has the form

$$Z^G(A)=-\prod_j\left[\frac{p_{aj}}{m_{aj}}\cdot\sigma_{\alpha_j\dot{\beta}_j}\delta_{\lambda_j\rho_j}\right]f^g(A), \tag{1}$$

where j runs over the edges of G and $f^G(A)$ is a function of the λ's, ρ's, and σ's, and of the scalar products of the vectors p_i and $e(\mu_{ik})$, which have components p_i^μ and

$$e(\mu_{ik})^\mu=\delta_{\mu_{ik}}{}^\mu,$$

respectively. The vector p_{aj} is the vector p_i associated with the vertex i on the leading end of line j. For a para-graph G the vector p_{aj} in (1) would be replaced by $(-p_{bj})$, where p_{bj} is the vector p_i associated with the vertex i on the trailing end of line j, and m_{aj} would be replaced by m_{bj}.

To recover from (1) the meson result (3.9) of paper I, but with the A of (3.9) now replaced by Z, one contracts, for each meson vertex i, the two spinor indices α_j and $\dot{\beta}_k$ associated with the lines j and k that terminate and originate on vertex i, respectively, against the two associated spinor indices α_j and $\dot{\beta}_k$ of the meson wave function $\psi^{\dot{\beta}_k\alpha_j}(s)=is\cdot\tilde{\sigma}^{\dot{\beta}_k\alpha_j}/\sqrt{2}$ corresponding to that vertex.

The variables in the set of variables A occurring in $Z^G(A)$ are arranged in one of the n standard linear orders corresponding to G. Such an ordering is obtained by dividing the set of variables A into the disjoint parts A_i associated with the various vertices i of G, and then ordering these parts A_i from right to left according to the order in which the corresponding vertices i of G are encountered by a path that starts just before some vertex of G and runs around the periphery of G, moving always in the direction of all the solitary quark lines and against the directions of all the paired quark lines. The set of variables A_i consists of the ordered set of variables

$$(p_i;\mu_{i1},\sigma_{i1};\ldots;\mu_{iL_i},\sigma_{iL_i})$$

followed by an ordered set of spin-flavor variables. These latter variables are the pairs of variables (α_j,λ_j) or $(\dot{\beta}_j,\rho_j)$ associated with the ends of those quarks lines j that terminate or originate on vertex i. They are ordered from right to left in the way in which the associated quark lines j are encountered by the peripheral path if it makes a small inward excursion around vertex i.

The set of quark variables (α_j,λ_j) in A_i, placed in the relative order in which they occur, in A_i, is written

$$(\alpha_{i1},\lambda_{i1};\ldots;\alpha_{iN_i},\lambda_{iN_i}). \tag{2a}$$

The set of antiquark variables $(\dot{\beta}_j,\rho_j)$ in A_i, placed in the relative order in which they occur in A_i, is written

$$(\dot{\beta}_{i\bar{N}_i},\rho_{i\bar{N}_i};\ldots;\dot{\beta}_{i1},\rho_{i1}). \tag{2b}$$

These equations define a labeling convention that will be used later.

By virtue of the ordering conventions established above the ordered set of arguments A_i in

$$Z^G(A_1,\ldots,A_n)\equiv Z^G(A)$$

determines G uniquely apart from the ortho-quark—para-quark specifications. The function $Z^{G'(A)}=Z(A)$ is the sum of the functions $Z^G(A)$ over all 2^N possible specifications of the ortho-quark—para-quark characters of the N quark lines of $G'(A)$, which is the graph without the ortho-quark—para-quark arrows.

There are n different standard linear orders of the n variables A_i associated with an n-vertex graph G. These are generated from any one of these orderings by the n cyclic permutations. In accordance with the spin-statistics theorem for physical particles the sign of $Z(A)$ depends on the relative order in which the baryon and antibaryon variables A_i occur in A: a cyclic permutation P of the n variables A_i of A that takes a single variable A_k from one end to the other of the linear sequence converts $Z(A)$ to

$$Z(PA)=\pm Z(A), \tag{3}$$

where the sign is plus if A_k is a meson or baryonium variable and minus if it is a baryon or antibaryon variable.

The minus sign appearing in (1) corresponds to any linear ordering of the variables A_i of A that is specified by breaking the cyclic order at a solitary quark line. Breaking at a pair of paired quark lines gives a plus sign.

III. THE ZERO-ENTROPY PART OF $M(A)$

The physical scattering function

$$M(A_1,\ldots,A_n)\equiv M(A)$$

corresponding to a set of n particles specified by the set of variables $(A_1,\ldots,A_n)$ is the connected part of the S-matrix element specified by these variables times

$$\left[(2\pi)^4\delta\left[\sum p_i\right]\right]^{-1}.$$

The zero-entropy part of $M(A)$ is given by the symmetrized sum of zero-entropy functions:

$$M^Z(A)=\sum_P \sigma(P)Z(PA)/n \ . \tag{4}$$

The sum is over all permutation operators P of the form

$$P=P_0\prod_{i=1}^{n_i}P_i \ , \tag{5}$$

where P_0 is any one of the $n!$ permutations of the order of the n variables A_i in A, and P_i is any one of the $\bar{n}_i$ permutations of the order of the quark and antiquark variables in A_i: a permutation P_i can permute the order of the quark variables in A_i and can permute the order of the antiquark variables in A_i, but it never interchanges quark variables with antiquark variables. Thus $\bar{n}_i\equiv\bar{n}(A_i)$ is 1, 6, 6, or 4 for a meson, baryon, antibaryon, or baryonium variable A_i, respectively. The function $Z(PA)$ is defined to be zero unless PA corresponds to some zero-entropy graph G of the kind shown in Fig. 4.

The number $\sigma(P)$ is the signature of the restriction of P_0 to baryon and antibaryon variables A_i: it is $+1$ or -1 according to whether the change produced by P_0 in the relative order of the baryon and antibaryon variables A_i in A is generated by an even or odd number of permutations of these variables.

For each permutation P_0 there is a set of n permutations that are generated from it by the n cyclic permutations. The $n!$ permutations P_0 can be expressed by writing $P_0=P_0''P_0'$ where P_0'' ranges over the n cyclic permutations and P_0' ranges over a set of $(n-1)!$ permutations P_0 not connected by cyclic permutations. The n contributions to (4) arising from a fixed P_0', but with different P_0'', are all equal, and hence one can restrict the sum in (4) to the sum over the $(n-1)!$ permutations P_0', and omit the factor n^{-1}. In this form of (4) there is one contribution from each cyclically ordered set of variables PA that corresponds to a zero-entropy graph of the kind shown in Fig. 4: the n different standard linear orders associated with a given graph G do not give separate contributions.

IV. PRODUCTS

The discontinuity around any physical-region singularity of any scattering function can be expressed as a linear combination of bubble-diagram functions M^B.[7,8] These functions are represented diagrammatically by bubble diagrams B of the kind shown in Fig. 5.

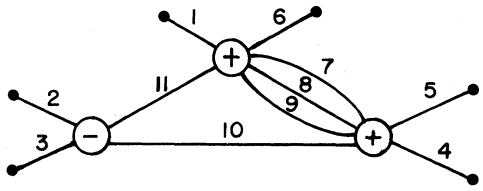

FIG. 5. A bubble diagram B.

Each plus bubble b of B is associated with a scattering function $M^b=M_+(A^b)$, where the n_b components A_i^b of A^b correspond one-to-one to the n_b edges of B that are incident upon b. Each minus bubble b of B is associated in the similar way with the function $M^b=M_-(A^b)$, which is the negative of the connected part of the matrix element of $S^\dagger$ specified by A^b, times

$$\left[(2\pi)^4\delta\left[\sum p_i\right]\right]^{-1} \ .$$

The plus-minus sign in $M_\pm(A^b)$ is often considered part of A^b. Then $M^b=M(A^b)$.

In general, a bubble diagram B is a Landau graph $g(B)$ with each internal vertex replaced by a plus or minus bubble. Each edge j of a Landau graph $g(B)$, or bubble diagram B, is associated with a particle-type label $t_j^{g(B)}\equiv t_j^B$. This type variable t_j^B is a partial characterization of A_j^B: it can place restrictions on ${p_j}^2$, on the (unordered set of) flavor variables, on the orbital variables μ_{jk} and σ_{jk}, and on the quark versus antiquark character of each spin-flavor label.

Each internal edge j of B connects a bubble $b'(j)$ of B to another bubble $b''(j)$, and defines a pairing of a component $A_{i'(j)}$ of $A^{b'(j)}$ with a component $A_{i''(j)}$ of $A^{b''(j)}$. For notational convenience the indices i are arranged so that $i'(j)=j$, where $p^0_{i'(j)}=p_j^0$ is positive.

The bubble-diagram function M^B corresponding to bubble diagram B is

$$M^B=\sigma^B\sum\!\!\!\!\!\!\int\left[\prod_{b\in B}M^b\right]H^B(n^B)^{-1}\omega^{g(B)} \ . \tag{6}$$

The factor $\omega^{g(B)}$ is the integrand of the integral that defines the phase-space factor $f^{g(B)}$ corresponding to the graph $g(B)$:

$$\omega^{g(B)}=\prod_j[(2\pi)\delta({p_j}^2-{m_j}^2)\theta(p_j^0)d^4p_j(2\pi)^{-4}]\prod_b{}'\left[(2\pi)^4\delta\left[\sum\epsilon_{bj}^{g(B)}p_j\right]\right] \ . \tag{7}$$

Here j runs over the set of internal edges of $g(B)$, and b runs over all but any one of the set of internal vertices of $g(B)$. The matrix elements ϵ^g_{bj} are matrix elements of the incidence matrix associated with graph g.

The function H^B has the form $H^B=\prod_j h_j^B/\bar{n}_j$ where j runs over the internal edges of B, and

$$h_j^B=\theta_j^B\prod_{k=1}^{L_j}(-g^{\mu_{i''(j)k}\mu_{jk}})\delta_{\sigma_{i''(j)k}\sigma_{jk}}\prod_{k=1}^{N_j}v_j\cdot\tilde{\sigma}^{\dot{\beta}_{i''(j)k}\alpha_{jk}}\delta_{\rho_{i''(j)k}\lambda_{jk}}\prod_{k=1}^{\bar{N}_j}v_j\cdot\tilde{\sigma}^{\dot{\beta}_{jk}\alpha_{i''(j)k}}\delta_{\rho_{jk}\lambda_{i''(j)k}}\ . \tag{8}$$

The function θ_j^B is unity if $L_j=L_{i''(j)}$, $N_j=\bar{N}_{i''(j)}$, $\bar{N}_j=N_{i''(j)}$, $p_j=-p_{i''(j)}$, and A_j^B conforms to the partial restrictions imposed by the type variable t_j^B. Otherwise θ_j^B is zero. The remaining symbols in (8) are defined in (2), or as in (2.18) of I, or by Kronecker.

The summation sign in (6) signifies a summation over the discrete indices occurring in H^B. For each of the upper spinor or vector indices of H^B there is, according to (2), an equal lower spinor or vector index in one of the functions M^b. Hence these sums constitute covariant contractions. Each flavor and σ index of H^B also is contracted with an identical flavor or σ index in one of the M^b.

To fix the sign σ^B in (6) the diagram B is drawn on a plane with no edges crossing through bubbles, and with the external edges of B extended out to a big circle that encloses B. The variables A_i^b or A_i^B occurring in the arguments of the individual functions $M(A^b)$ or in the arguments of the bubble diagram function M^B itself are ordered from right to left according to the sequence in which the associated vertices i are encountered by a path that starts at the top of the bubble or big circle and proceeds clockwise. The sign σ^B is then a product of factors (-1), one for each crossing of a pair of fermion edges in this diagrammatic representation of B.

The factor n^B in (6) is the symmetry number of the bubble diagram B: it is the number of distinct permutations

$$\pi:(b,j)\rightarrow(\pi b,\pi j)$$

on the bubbles b and *internal* edges j of B that leave B unchanged in the sense that if $\epsilon_{b,j}^{g(B)}=\epsilon_{b,j}^B$ are the elements of the incidence matrix of the graph $g(B)$, and σ_b^B is the sign of bubble b of B, then the following invariance conditions hold:

$$\epsilon_{\pi b,\pi j}^B=\epsilon_{b,j}^B \quad (\text{all } b \text{ and } j)\ , \tag{9a}$$

$$\sigma_{\pi b}^B=\sigma_b^B \quad (\text{all } b)\ , \tag{9b}$$

and

$$t_{\pi j}^B=t_j^B \quad (\text{all } j)\ . \tag{9c}$$

Two bubble diagrams B' and B'' are topologically equivalent if and only if there is a permutation π of the bubbles b and internal edges j of B' such that

$$\epsilon_{\pi b,\pi j}^{B'}=\epsilon_{b,j}^{B''} \quad (\text{all } b \text{ and } j)\ , \tag{10a}$$

$$\sigma_{\pi b}^{B'}=\sigma_b^{B''} \quad (\text{all } b)\ , \tag{10b}$$

and

$$t_{\pi j}^{B'}=t_j^{B''} \quad (\text{all } j)\ . \tag{10c}$$

The discontinuity formulas[7-9] specify that there is only one contribution from each set of topologically equivalent bubble diagrams: two topologically equivalent bubble diagrams B' and B'' do not give additive contributions $M^{B'}$ and $M^{B''}$ to the discontinuity.

The sign σ^B was fixed by drawing B with the edges j incident upon each bubble b ordered in some definite way. A change in these orders gives a topologically equivalent diagram B that gives no additional contribution to the discontinuity.

A *fully labeled* bubble diagram $\bar{B}$ compatible with a bubble diagram B is a diagram that can be constructed by assigning to the end $i'(j)$ of each internal edge j of B a set of variables $A_{i'(j)}^{\bar{B}}$, assigning to the end $i''(j)$ of each internal edge j of B a set of variables $A_{i''(j)}^{\bar{B}}$, where $A_{i'(j)}^{\bar{B}}$ and $A_{i''(j)}^{\bar{B}}$ must be such that $\theta_j^B\neq 0$, and assigning a set of variables A_e^B to both ends of each external edge e of B. Two fully labeled bubble diagrams $\bar{B}'$ and $\bar{B}''$ are topologically equivalent if and only if there is a permutation π of the bubbles b and internal edges j of $\bar{B}'$ such that

$$\epsilon_{\pi b,\pi j}^{\bar{B}'}=\epsilon_{b,j}^{\bar{B}''} \quad (\text{all } b \text{ and } j)\ , \tag{11a}$$

$$\sigma_{\pi b}^{\bar{B}'}=\sigma_b^{\bar{B}''} \quad (\text{all } b)\ , \tag{11b}$$

$$A_{i''(\pi j)}^{\bar{B}'}=A_{i''(j)}^{\bar{B}''} \quad (\text{all } j)\ , \tag{11c}$$

and

$$A_{i'(\pi j)}^{\bar{B}'}=A_{i'(j)}^{\bar{B}''} \quad (\text{all } j)\ . \tag{11d}$$

The sums and integrals that occur in the definition (6) of M^B can be regarded as a summation over the fully labeled $\bar{B}$ compatible with B. If the variables p_j associated with the lines j of $\bar{B}$ are all different, as they are on all but a set of zero measure, then M^B contains the contributions from n^B topologically equivalent fully labeled diagrams $\bar{B}$. These n^B contributions are all equal. Thus the factor $(n^B)^{-1}$ in (6) can be replaced by a factor $\theta^{\bar{B}}$ that takes on values 0 or 1 (except on sets of zero measure) in such a way as to allow a nonzero contribution from only one of any set of topologically equivalent $\bar{B}$. On the set of zero measure $\theta^{\bar{B}}$ is the inverse of the number of permutations π that leave $\bar{B}$ unchanged. Thus, apart from this minor

complication on sets of zero measure, the contribution to the discontinuity associated with B is simply a sum over any complete set of topologically inequivalent fully labeled bubble diagrams $\bar{B}$ compatible with B:

$$M^B=\sigma^B\sum_{\bar{B}\subset B}\prod_b M^{b(\bar{B})}\prod_j\left[h_j^{\bar{B}}/\bar{n}_j\right]\theta^{\bar{B}}\omega^{\bar{B}}\,, \qquad (6')$$

where the bubble diagram B is considered here to be a symbolic representation for the set of $\bar{B}$ compatible with B, and a sum-integral over $\bar{B}$ is a sum over the discrete variables associated with the internal edges j of the labeled diagram $\bar{B}$ and an integral over the momentum-energy variables

$$p_j=p_{i'(j)}=-p_{i''(j)}$$

associated with the internal edges j of $\bar{B}$. The factor $\omega^{\bar{B}}$ is the factor represented by $\omega^{g(\bar{B})}$ in (6) and (7).

The above discussion specifies the sign and symmetry factors connected with the usual bubble diagram functions M^B. Let Z^B denote the part of M^B that arises from the zero-entropy parts of the functions M^b associated with the bubbles b of B. The function Z^B is obtained by replacing each factor $M^b=M(A^b)$ in M^B by its zero-entropy part $M^Z(A^b)$ defined in (4).

The sum in (4) over the permutations P includes a sum over the $\bar{n}_j$ permutations $P_i=P_{i'(j)}=P_j$ in (5). This latter sum converts the P_i in P in (4) to a factor

$$\sum_{k=1}^{\bar{n}_j}P_{jk}\,. \qquad (12a)$$

This factor stands on one side of the metric matrix h_j^B in (8). On the other side stands a similar factor

$$\sum_{k=1}^{n_j}P_{i''(j)k}\,, \qquad (12b)$$

which can be commuted through h_j^B and combined with the factor (12a) to give just $\bar{n}_j$ times this factor (12a). The extra numerical factor $\bar{n}_j$ cancels against the factor $\bar{n}_j^{-1}$ that occurs in (6') to give for the net result precisely the factor (12a), which stands together with h_j^B between the two zero-entropy functions. Thus, for example, the baryon connection represented by the top-left diagram in Fig. 6 can be replaced by the sum of the quark connections represented by the rest of Fig. 6, provided each line segment on the right-hand side of the second equation in Fig. 6 is considered to represent now the product of a flavor δ function and a spin metric factor $v\cdot\tilde{\sigma}$.

The baryon connection j thus gives a sum over the 3! ways of joining the three quark lines that come into vertex $i'(j)$ [or $i''(j)$] to the three quark lines that leave vertex $i''(j)$ [or $i'(j)$]. Of course, some or all of these 3! terms may give a null contribution, due, for example, to a mismatching of the flavors of the two quarks on the two ends of one or more of the connecting quark segments in Fig. 6: the Kronecker delta functions $\delta_{\lambda\rho}$ in h_j^B cause the vanishing of a contribution in which any two such flavors differ.

It should be noted that our normalization of $M(A^b)$ corresponds to a normalization of the corresponding S matrix $S(A^b)$ that leaves out the traditional factor $(n_j)^{-1/2}$ associated with n_j identical quarks (or antiquark) in particle j. This factor is absorbed instead into the normalization factor $\bar{n}_j$ appearing in H^B. Then the identical-quark case can be treated together with the nonidentical-quark case, without special consideration.

Consider now a contribution to Z^B corresponding to some $\bar{B}$ in which all the labels p_j are different. The set of edges incident upon any bubble b of $\bar{B}$ can be arranged in some definite order and there will be [in the θ form (6') of M^B] a nonzero contribution from only this one way of connecting the particle edges j to the bubbles b of B. However, the sum in (4) over the $(n_b-1)!$ permutations P_0' associated with bubble b gives a term $Z(PA^b)$ for each of the $(n_b-1)!$ different cyclic orders of the set of variables A_i^b. Some of these orders may give a null contribution, because only certain orderings of variables correspond to allowed zero-entropy graphs (see Fig. 4). Thus the sum generated by the permutations P_0' associated with the fixed bubble b can be restricted to a sum over those different cyclic orderings of the variables A_i^b that correspond to a zero-entropy graph $G(PA^b)$. For each bubble b of B there is a sum of this kind. Thus the contribution to M^B from terms

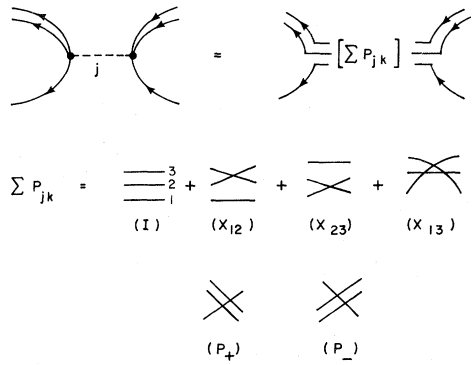

FIG. 6. Diagrammatic representation of the sum of quark-edge connections entailed by a baryon connection j. The factor $\sum P_{jk}$ stands together with h_j^B between the two zero-entropy functions.

corresponding to the fixed $\bar{B}$ is just a sum over terms corresponding to any complete set of topologically inequivalent quark graphs $\bar{g}$ compatible with B. And the full function Z^B is a sum-integral over any complete set of topologically inequivalent fully labeled particle-quark graphs $\bar{g}$ compatible with B. The concepts just introduced are not defined.

A particle-quark graph $\bar{g}$ compatible with B is a graph $\bar{g}$ that can be formed by replacing each bubble b of B by a quark graph $G^b(\bar{g})$, with each edge of B that is incident upon b connected in $\bar{g}$ to a different vertex i of $G^b(\bar{g})$ (see Fig. 7). The number of quark lines originating and terminating on this vertex i of $G^g(\bar{g})$ must accord with the type t_j^B or t_e^B of edge j or e of B. This is illustrated in the top-left diagram of Fig. 6, for the case of a baryon edge j.

A *fully labeled* graph $\bar{g}$ compatible with B is a particle-quark graph compatible with B that has a label $A_i^{\bar{g}}$ attached to each quark vertex i, with the labels $A_{i'(j)}^{\bar{g}}$ and $A_{i''(j)}^{\bar{g}}$ restricted by the condition that $\theta_j^B \neq 0$. Two such fully labeled graphs $\bar{g}'$ and $\bar{g}''$ are topologically equivalent if and only if there is a permutation

$$\pi:(i,j,k)\rightarrow(\pi i,\pi j,\pi k)$$

of the internal vertices i of $\bar{g}'$, the internal particle edges j of $\bar{g}'$, and the quark lines k of $\bar{g}'$ such that

$$\epsilon_{\pi i,\pi j}^{\bar{g}'} = \epsilon_{i,j}^{\bar{g}''} \quad \text{(all } i \text{ and } j\text{)}, \tag{13a}$$

$$\epsilon_{\pi i,\pi k}^{\bar{g}'} = \epsilon_{i,k}^{\bar{g}''} \quad \text{(all } i \text{ and } k\text{)}, \tag{13b}$$

$$\sigma_{\pi i}^{\bar{g}'} = \sigma_i^{\bar{g}''}, \tag{13c}$$

and

$$A_{\pi i}^{\bar{g}'} = A_i^{\bar{g}''} \quad \text{(all } i\text{)}. \tag{13d}$$

Here $\sigma_i^{\bar{g}}$ is the sign of the bubble in which vertex i lies.

The result stated above combined with that expressed by Fig. 6 entails that

$$Z^B = \sigma^B \sum\!\!\!\!\!\!\int_{\bar{g}\subset B} H^{\bar{g}} \prod_b Z^{G^b(\bar{g})} \theta^{\bar{g}} \omega^{\bar{g}}, \tag{14}$$

where the sum-integral is over all fully labeled graphs $\bar{g}$ compatible with B: it is a sum over the different (unlabeled) graphs $\bar{g}$ compatible with B, a sum over the discrete indices of $A_{i'(j)}$ and $A_{i''(j)}$ associated with the internal particle edges j of $\bar{g}$, and an integral over the momentum-energy vectors

$$p_j = p_{i'(j)} = -p_{i''(j)}$$

associated with the internal particle edges j of $\bar{g}$. The function $\theta^{\bar{g}}$ is zero or one (except on a set of zero measure) in such a way as to allow precisely one contribution from any set of fully labeled graphs $\bar{g}$ that are topologically equivalent. The factor $\theta^{\bar{g}}$ can be replaced by the inverse of $n^{\bar{g}}$, which is the number of permutations

$$\pi(i,j,k)\rightarrow(\pi i,\pi j,\pi k)$$

that satisfy (13) with $\bar{g}'$ and $\bar{g}''$ replaced by $\bar{g}$. This latter form correctly weights the sets where two p_j's coincide.

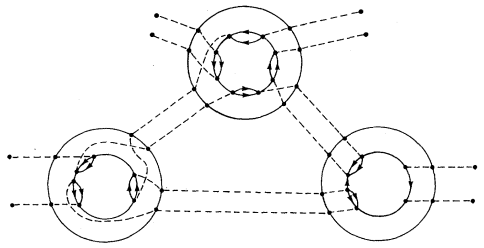

FIG. 7. A particle-quark graph $\bar{g}$ representing a typical contribution to Z^B. The three outer circles represent the bubbles b of B. Each encloses a graph that represents a contribution $Z(PA^b)$ to $M^Z(A^b)$.

The factor $H^{\bar{g}}$ in (14) is

$$H^{\bar{g}} = \prod_j \left[h_j \sum_{k=1}^{n_j} P_{jk} \right] \prod_e \left[\sum_{k=1}^{n_e} P_{ek} \right], \tag{15}$$

where j and e run over the internal and external particle edges of $\bar{g}$, respectively. The factors P_{jk} and P_{ek} in (15) are operators whose action is now described.

The set of variables A_j includes the set

$$a_j = (a_{j1}, \ldots, a_{jN_j})$$

of spin-flavor indices, the set

$$\sigma_j = (\sigma_{j1}, \ldots, \sigma_{jL_j})$$

of σ indices, and the set

$$\mu_j = (\mu_{j1}, \ldots, \mu_{jL_j})$$

of orbital indices. The permutation $P_{jk} = P$ is specified by a permutation

$$P:(1, \ldots, N_j)\rightarrow(P1, \ldots, PN_j)$$

of the set of N_j integers. For example, if $P_{jk} = P$ is the permutation P_- represented by the last diagram of Fig. 6, then

$$(P1,P2,P3) = (3,1,2).$$

If j is a baryon edge, then each index σ_{jk} is two valued and these two values together with a sequence $(P1, \ldots, P3)$ designate two orthonormal vectors

$$|\sigma,(P1,P2,P3)\rangle=\begin{cases}\dfrac{|p1\rangle-|p3\rangle}{\sqrt{2}} & (\sigma=1)\,,\\ \dfrac{2|P2\rangle-|P1\rangle-|P3\rangle}{\sqrt{6}} & (\sigma=2)\,,\end{cases} \tag{16}$$

where $\langle n\,|\,m\rangle=\delta_{nm}$ for any integers n and m. If j is a baryonium edge, then each index σ_{jk} is three valued, and for each permutation $(P1,P2,P3,P4)$ of the four integers (1,2,3,4) an orthonormal set of three vectors is defined:

$$|\sigma,(P1,P2,P3,P4)\rangle=\begin{cases}\dfrac{|P1\rangle-|P2\rangle}{\sqrt{2}} & (\sigma=1)\,,\\ (|P1\rangle+|P2\rangle-|P3\rangle-|P4\rangle)/2 & (\sigma=2)\,,\\ \dfrac{|P3\rangle-|P4\rangle}{\sqrt{2}} & (\sigma=3)\,.\end{cases} \tag{17}$$

The permutation operator $P_{jk}=P$ acts in the space associated with the variables (a_j,σ_j), and has matrix elements

$$P(a_j,\sigma_j;a_j',\sigma_j')=\prod_{i=1}^{N_j}\langle a_{j,Pi}\,|\,a_{ji}'\rangle\prod_{i=1}^{L_j}\langle\sigma_{ji},(1,\ldots,N_j)\,|\,\sigma_{ji}',(P1,\ldots,PN_j)\rangle\,, \tag{18}$$

where $\langle a\,|\,a'\rangle=\delta_{aa'}$. The operator P_{jk} in (14) acts on $M^{b'(j)}(A_j)$ as follows:

$$P_{jk}M^{b'(j)}(p_j,a_j,\sigma_j,\mu_j)=P_{jk}(a_j,\sigma_j;a_j',\sigma_j')M^{b'(j)}(p_j,a_j',\sigma_j',\mu_j)\,, \tag{19}$$

where a sum over the repeated indices a_j' and σ_j' is implied.

The operators P_{ek} are defined analogously.

This concludes the description of the sign, symmetry, and statistical factors in the bubble-diagram functions M^B, and in the parts Z^B of these functions that arise from the zero-entropy contributions to the scattering functions M^b corresponding to their bubbles b.

V. PARTICLE VARIABLES

The sum of permutation operators P_{jk} occurring in (15) can be written

$$\sum_{k=1}^{n_j}P_{jk}=n_j\hat{P}_j\,, \tag{20}$$

where $\hat{P}_j$ is a projection operator onto a symmetrized subspace of the space spanned by the vectors $|a_j,\sigma_j\rangle$. The projection operator $\hat{P}_j$ can be written in the form

$$\hat{P}_j=\sum_{\hat{a}_j}|\hat{a}_j\rangle\langle\hat{a}_j|\,, \tag{21}$$

where $\hat{a}_j$ is a set of indices that labels the vectors of an orthonormal basis of the symmetrized subspace.

The part of the integrand of (14) that is associated with edge j of B is

$$\begin{aligned}Z^{G^{b''(j)(\bar{g})}(A^{b''(j)}(\bar{g}))}h_j\textstyle\sum P_{jk}Z^{G^{b'(j)(\bar{g})}(A^{b'(j)(\bar{g})})}&\equiv\langle Z_j''\,|\,a_j',\sigma_j'\rangle\langle a_j',\sigma_j'\,|\,h_j\,|\,a_j,\sigma_j\rangle\langle a_j,\sigma_j\,|\,\textstyle\sum P_{jk}\,|\,Z_j'\rangle\\ &=\langle Z_j''\,|\,h_jn_j\hat{P}_j\,|\,Z_j'\rangle\\ &=\sqrt{n_j}\langle Z_j''\,|\,h_j\hat{P}_j\,|\,Z_j'\rangle\sqrt{n_j}\\ &=\sqrt{n_j}\langle Z_j''\,|\,\hat{P}_jh_j\hat{P}_j\,|\,Z_j\rangle\sqrt{n_j}\\ &=\sqrt{n_j}\langle Z_j''\,|\,\hat{a}_j\rangle\langle\hat{a}_j\,|\,h_j\,|\,\hat{a}_j\rangle\langle\hat{a}_j\,|\,Z_j'\rangle\sqrt{n_j}\,.\end{aligned} \tag{22}$$

The result of applying this transformation of variables to each edge j and e takes (14) to the form

$$\hat{Z}^B=\sigma^B\sum_{\bar{g}CB}\prod_b\left[\hat{Z}^{G^b(\bar{g})}\right]\hat{H}^{\bar{g}}\hat{\theta}^{\bar{g}}\omega^{\bar{g}}\,, \tag{23}$$

where the carets on $\hat{Z}$, $\hat{H}$, and $\hat{\sigma}$ indicate that the variables (a_j,σ_j) are replaced by the variables $\hat{a}_j$. Moreover, a factor $\sqrt{n_j}$ for each edge j of B incident upon b has been introduced into $\hat{Z}^{G^b(\bar{g})}$.

The orbital quantum numbers in $\hat{A}_j=(p_j,\mu_j,\hat{a}_j)$ are separate from the spin quantum numbers that occur in $\hat{a}_j$. Rest-frame Clebsch-Gordan combinations gives states of definite J, which are precisely the particle states of the constituent-quark model.[10] Boosts from the rest frame give covariant forms of the $h_j^{\bar{g}}$ for states of fixed J. Use of these variables gives an alternative form of (23):

$$\tilde{Z}^B=\sigma^B\sum_{\bar{g}CB}\prod_b\tilde{Z}^{G^b(\bar{g})}\tilde{H}^{\bar{g}}\tilde{\theta}^{\bar{g}}\omega^{\bar{g}}\,, \tag{24}$$

where the tilde over $\tilde{Z}$, $\tilde{H}^B$, and $\tilde{\sigma}^{\bar{g}}$ signifies the use of the variables $\tilde{A}_j$ of the constituent-quark model.

The functions $\tilde{Z}^{G^b(\bar{g})}$ depend on the quark diagram $G^b(\bar{g})$, and hence on the order of the variables, $\tilde{A}_i^b$ in $\tilde{A}^b$. But, in contrast to the case of the zero-entropy functions $Z^{G^b(\bar{g})}$, the individual variables $\tilde{A}_i^b$ occurring in the argument of $\tilde{Z}^{G^b(\bar{g})}$ do not specify, for example, which of the three flavors is to be assigned to the solitary quark edge incident upon a baryon vertex i of $\bar{g}$.

In principle the intermediate particles occurring in (24) include only the stable parameters, but important cut contributions can often be simulated by contributions from poles lying close to the physical region.

VI. TOPOLOGICAL EXPANSION *A*

By virtue of the cyclic ordering of the variables associated with any zero-entropy function $Z^{G^b(\bar{g})}$, $\hat{Z}^{G^b(\bar{g})}$, or $\tilde{Z}^{G^b(\bar{g})}$, a topological expansion essentially identical to that of paper I can be introduced. This expansion is defined by specifying that the zero-entropy quark graphs $G^b(\bar{g})$ be placed on an oriented surface Σ with the directions of all solitary quark lines agreeing with the direction induced by the orientation of Σ, and with the directions of all paired quark lines opposing the direction induced by the orientation of Σ. The orientation of Σ as represented on paper is taken to be clockwise (see Fig. 7).

All quark-particle graphs $\bar{g}$ formed by connecting zero-entropy graphs G by particle lines in the manner discussed in the preceding section are then classified by their boundary structure and topological index $\lambda(\bar{g})$.

The boundary structure is specified by a decomposition of the external particle edges into a set of cyclic sets corresponding to the set of boundaries of $\bar{g}$. The topological index is given by

$$\lambda(\bar{g})=e(\bar{g})-v(\bar{g})-\omega(\bar{g})+1\,, \tag{25a}$$

where e, v, and ω stand for numbers of edges, vertices, and windows of the graph, or equivalently by

$$\lambda(g(\bar{g}))=e(g(\bar{g}))-v(g(\bar{g}))-\omega(g(\bar{g}))+1\,, \tag{25b}$$

where $g(\bar{g})$ is the Landau graph obtained by contracting to point vertices the quark graphs $G^b(\bar{g})$ but retaining the cyclic order in which the edges are incident upon these vertices. The boundary structure and topological index together is denoted by $\tau(\bar{g})$.

The topological expansion asserts that M can be decomposed into a sum of terms M^τ corresponding to different topological types τ, and that when any equation $X=0$ derived solely from unitarity and cluster decomposition is separated into parts of different topological character, then each such part of the equation is separately satisfied:

$$X=\sum X^\tau=0 \text{ implies } X^\tau=0 \text{ (all } \tau)\,. \tag{26}$$

No cancellations among the parts X^τ of different topological type τ are required.

The "ordered amplitudes" are the parts M^τ corresponding to $\lambda=0$ and a single boundary. The constituent-quark-model particle variables $\tilde{A}_i$ can be used. The ordered amplitudes satisfy the closed, planar discontinuity formulas: their discontinuity formulas are the same as those of the physical scattering functions except that the contribution M^B associated with bubble diagram B is reduced to a sum of terms corresponding to the different ways the Landau graph $b(B)$ can be drawn as a planar graph $g_p(B)$, and for each such term the scattering function M^b associated with bubble b of B is replaced by the ordered amplitude specified by the cyclic order in which the lines of $g_p(B)$ enter vertex b.

Summation of the ordered amplitudes associated with any process gives the planar amplitude, which is the first approximation to the physical scattering function. The situation is essentially identical to that described by Chew and Rosenzweig.[11]

Pure baryonium states do not couple to pure meson states at the planar level, and hence the planar baryonium Regge trajectories are distinct from the planar meson trajectories. The selection rule forbidding baryonium-meson transitions arises from the fact that in the particle graphs $g(\bar{g})$ the meson

edges connect only to each other and to the left-hand sides of the (directed) baryon lines, whereas baryonium edges connect only to each other and to the right-hand sides of baryon lines.

As in the meson sector the ordered amplitudes M^{τ} are not equal to the zero-entropy functions $\tilde{Z}^{G^b}$. In the meson sector the ortho-quark—para-quark transitions were considered elements of complexity, and the zero-entropy amplitudes corresponded to the planar graphs $\bar{g}$ having no such transitions. In the general hadron case there is an added element of complexity associated with the crossings of quark lines illustrated by the last five terms in Fig. 6. Thus in the general case the zero-entropy amplitudes correspond to the graphs [$\bar{g}$ or $g(\bar{g})$] having one boundary, topological index zero, no ortho-quark—para-quark transitions, and no quark-line crossings.

The zero-entropy level is also a closed, planar level: the discontinuity formulas for the zero-entropy functions are identical to those for the physical scattering functions except that the discontinuities associated with nonplanar Landau graphs are zero and the discontinuity formulas associated with planar Landau graphs have, throughout, zero-entropy amplitudes in place of physical scattering amplitudes. The spin factors factor out.

In specifying the ordered level of the topological expansion, and all higher-order levels, the topological character of a contribution is completely characterized by the boundary structure and topological index λ of the associated graph $\bar{g}$, or $g(\bar{g})$. For specifying the zero-entropy level one must assign an ortho-quark or para-quark character ϵ_b to each quark line of $\bar{g}$, and a permutation P_{jk} to each internal particle edge j of $\bar{g}$, or $g(\bar{g})$. This latter permutation is presented diagrammatically by "thickening" the particle edge into a ribbon lying on Σ, and drawing on this ribbon the appropriate permutation, as illustrated in Fig. 6.

The zero-entropy amplitudes are distinguished from the ordered amplitudes in several ways. Each "particle" j at the zero-entropy level is identified by a set of variables A_j in which the linear order of the spin-flavor variables is fixed. At the ordered level each basic particle is specified by a set of variables that specifies a particle of the constituent quark model, and these latter particles are invariant under permutations of the quarks (and likewise the antiquarks) in the particle. On the other hand, the portion of any boundary or orbit lying between two vertices has a single well-defined flavor for any graph $\bar{g}$ corresponding to a zero-entropy amplitude, whereas for graphs $\bar{g}$ corresponding to ordered amplitudes flavor is not necessarily conserved on the boundary in this way.

VII. TOPOLOGICAL EXPANSION *B*

To construct a topological expansion that isolates the zero-entropy functions one proceeds as follows. Start with a set of zero-entropy quark graphs G_i of the kind shown in Fig. 4(a). Each quark edge is assigned an ortho-character or para-character, a flavor, and also a color 1, 2, or 3. Each solitary quark line has color 1, and each paired quark line has color 2 or 3 according to whether it is an internal or peripheral line in the graph G_i.

These graphs G_i are joined together by particle edges. Each of these connecting particle edges is decomposed into a sum of contributions of the kind illustrated in Fig. 6. These connecting particle edges are now contracted to points. Each of these points is a *junction vertex,* where two graphs G_i meet. The quark graph formed in this way is $G = G_n \cdots G_2 G_1$.

Each junction vertex V is associated with a permutation P_V. This permutation defines a separation of the quark edges incident upon V into a set of *associated pairs:* each quark edge incident upon V and lying in one of the two quark graphs G_i that meet at V is *associated* with a quark edge incident upon V and lying in the other G_i.

The permutation I (see Fig. 1) is the identity permutation. A junction vertex V is a *removable vertex* if and only if (1) $P_V = I$ and (2) in each associated pair of quark edges incident upon V either both edges have ortho-character or both have para-character (i.e., none of the 2, 3, or 4 quark lines passing through V has an ortho-para transition), and, moreover, both of these edges have the same flavor.

A removable vertex V of G can be *removed.* In this process each associated pair of quark edges incident upon V is replaced by a single quark edge. The color, flavor, and ortho-para character of each new single quark edge is the same as these characteristics of either one of the two quark edges that it replaces.

Let G'' be the quark graph obtained from G by removing all removable vertices. Then $F(G'',p) = \pm F(G,p)$: The spinor function associated with G'' is the same as the spinor function associated with G, up to a sign. (This change of sign is the same as the change of the sign associated with the order of the fermion variables.) Let G''' be G'' minus lines incident on no vertex, with a P_V for each junction V, and a flavor, color, and ortho-para label for each edge.

Let G' be the graph obtained from G by cutting each nonremovable vertex V in two, in the way that separates the two graphs G_i that meet there. Let G'_j, $j \in (J)$, be the connected parts of G'. Let g'_j be

the particle graph associated with G_j'. It can be constructed by replacing each subgraph G_i of G_j' by the particle-quark graph $\bar{g}(G_i)=\bar{g}_i$, thereby replacing G_j' by $\bar{g}(G_j')=\bar{g}'_j$, and then taking its particle subgraph $g(\bar{g}'_j)=g'_j$. Alternatively, one may replace each removable vertex of G_j' by a particle line and then contract each graph G_i to a point.

The topological class of G is defined by the quark graph G''' and the set of topological indices $\gamma(g'_j)$, $j\in(J)$.

This topological classification uses only the planar graphs G_i. One can, of course, give an equivalent formulation in terms of the feathered surface associated with the graph $\hat{g}(G)$ (see Fig. 4). Then the two colors 2 and 3 can be considered to identify quark lines that lie, respectively, above and below the plane containing both the junction lines and the quark lines with color 1. The symmetry between 2 and 3 is then displayed more graphically.

VIII. CONNECTION TO RECENT WORKS

The foregoing parts of this paper were written earlier,[14] but were not then submitted for publication because of uncertainty as to whether the formalism could be successfully applied to physics: in spite of the automatic occurrence of the $SU(6)_w$ and quark-model symmetries at low levels of the topological expansion it was not clear whether the theory as a whole could agree with experiment.

One concern was that the value of the universal strong-interaction coupling constant was fixed in principle by nonlinear conditions, but it was not known whether a calculation would yield a value anywhere close to the empirical one. Recently, however, Espinosa,[15] working under the guidance of Chew, has completed several different calculations, based on several different approximations, and the agreement between the calculated and experimental values of g^2 is within a factor of 2.

A second concern arose from the fact that the part of the propagators that contributes to the zero-entropy amplitudes is small, particularly for baryons and baryonium, and this smallness creates the possibility that the zero-entropy amplitudes might be useless, either as a basis for practical calculations, or even as a basis for understanding the approximate symmetries of physical amplitudes. In previous works[11] based on the topological approach it could be argued that the planar amplitudes were a large part of the whole. This property is not shared by the zero-entropy amplitudes, and it appeared that it would be necessary to treat these amplitudes not as reasonably good first approximations but more like the fundamental point interactions of local field theory. However, it was not known exactly how to combine the nonperturbative conditions on zero-entropy amplitudes with a perturbative expansion for higher-order corrections. Nor was it clear whether such a procedure would allow any significant remnant of the low-order symmetries to propagate to the physical level.

These questions have now been examined in some detail by Chew and Levinson, with encouraging results. The central idea of the Chew-Levinson paper[16] is to construct a Feynman-type expansion of the scattering function that associates the vertices of the graphs not with the point-coupling polynomials of local field theory but rather with the zero-entropy amplitudes. To obtain a one-to-one correspondence between the particle-quark graphs of the topological expansion and corresponding Feynman-type functions a particle contraction rule is introduced. This rule specifies that any zero-entropy subgraph should be contracted to a point vertex.

In a particle-quark graph each particle line l_i of the Feynman graph is replaced by a set s_i consisting of this particle line l_i and its associated set of 2, 3, or 4 quark lines. When all zero-entropy parts are contracted to points no particle line l_i, or its associated set s_i, remains unless this set s_i is such that either (1) some quark line of s_i has an ortho-quark—para-quark transition (of the kind discussed in paper I), (2) some pair of quark lines of s_i undergoes a color switch (of the kind illustrated by the crossed-line contributions of Fig. 6), or (3) neither of the above two conditions holds, but the particle line l_i of s_i begins and ends at the same vertex V, and it enters and leaves V along nonadjacent line segments of the set of cyclically ordered end segments of lines l_i incident upon V.

Chew[17] has argued that any graph containing a set s_i satisfying the condition (3) stated above should be classified as a weak-interaction graph. Then each of the remaining "strong-interaction" graphs has a different topological character, and its topological type is uniquely specified by the (partially contracted) particle-quark graph with ortho-quark—para-quark transitions and color switches displayed. Consequently the topological expansion at the strong-interaction levels becomes identical to the expansion in terms of these partially contracted particle-quark graphs.

The Chew-Levinson rules for this graphical expansion differ from the Feynman rules in the following ways: (1) the vertices correspond to zero-entropy amplitudes, rather than polynomials; (2) each line l_i of the Feynman graph is replaced by the set s_i consisting of l_i and its set of 2, 3, or 4 associated quark lines; (3) each such set s_i has some element of complexity (either an ortho-quark—para-quark transition or a color switch); (4) each vertex is an or-

dered vertex—the cyclic order of the particle and quark lines incident upon a vertex determines the associated zero-entropy function; and (5) certain normalization factors are different from Feynman's.

The unusual normalization factors mentioned in point (5) are demanded by the required compatibility of the S-matrix discontinuity formulas with the topological expansion. They consist of unorthodox factors of 2 in the normalizations of spin states and propagators. These factors arise from the topological independence of the ortho-quarks, and para-quarks.

To understand the origin of these factors of 2 one may recall that the purpose of paper I was to ensure the solubility of the spin-dependent aspects of the duality conditions in a trivial way by the introduction of spin factors analogous to the Chan-Paton factors for isospin. The conditions allowed two different solutions—the ortho-amplitudes and the para-amplitudes. The normalizations of these ortho-amplitudes and para-amplitudes were fixed by the requirement that they be *additive* contributions to the full amplitude: the full amplitude was separated into a *sum* of terms associated with different topologies, and the ortho-amplitude and para-amplitude contributions were defined to be topologically different. With the normalizations fixed in this way the zero-entropy amplitudes each satisfy planar-type discontinuity equations: their discontinuity equations are identical to those of physical scattering functions except that their singularities are associated only with planar diagrams, and in each planar-diagram discontinuity formula each of the usual physical scattering amplitudes is replaced throughout by appropriate zero-entropy amplitudes.

By virtue of these normalization conventions one must, in the construction of the full amplitude, simply add together the ortho-quark and para-quark contributions: one cannot introduce any extra normalization factor without disrupting the condition that the whole amplitude be the sum of the topologically different parts.

The normalizations of the contributions of the zero-entropy functions to the discontinuities of physical amplitudes are fixed by Eq. (4), which defines the zero-entropy part of any M function occurring in a discontinuity equation to be a sum of all zero-entropy functions compatible with the set of physical particles associated with M, and by (6), which defines the bubble diagram functions from which the discontinuity equations are constructed. Each function $Z(PA)$ occurring to (4) is a sum of the 2^N zero-entropy functions corresponding to the independent selection of the ortho-propagator or para-propagator for each of the N quark lines of $G'(A)$.

Each intermediate particle line l_i of a bubble diagram can be replaced by the corresponding set of s_i of particle and quark lines. Then each intermediate quark line q_j runs between two bubbles. The zero-entropy part of the M function represented by any bubble is represented by a point vertex in the partially contracted particle-quark graphs. This point vertex can be "decontracted" into the sum of particle-quark graphs $\bar{g}(G_i)$ of Fig. 4 that represents this zero-entropy part. In this sum each quark line of the graphs $\bar{g}(G_i)$ occurs as a sum of an ortho-quark and a para-quark line. Thus the intermediate line q_j can plug independently on either end into either an ortho-quark or para-quark line of some $\bar{g}(G_i)$. This gives a sum of four terms.

In the original two-component formalism all four terms run through the same two-by-two spin factor $v\cdot\tilde{\sigma}$ of Eq. (8). But in the four-component formalism the ortho-quark and para-quark parts are joined together to form the lower and upper halves of one four-component vector. Thus in the four-component formalism the four terms run through four separate two-by-two submatrices of the four-by-four Dirac matrix associated with the intermediate quark line.

In the intermediate-particle rest frame, where the matrices $v\cdot\tilde{\sigma}$ in (8) are unit matrices, the intermediate four-by-four Dirac matrix is just $1+\beta$: it is the four-by-four matrix that has a two-by-two unit matrix in each of the four corners.

The transformation from the two-component to four-component formalism was described in detail for mesons in Appendix C of paper I. That conversion exploited the fact that the coefficients for combining a quark and an antiquark into a vector or scalar meson were given by the Pauli matrices $\sigma_\mu^{\alpha\beta}/\sqrt{2}$. In the more general situation encountered here one must use general Clebsch-Gordan coefficients.

To convert to the four-component formalism in the general case one may treat each quark line separately. If one uses the expressions $p_a\cdot\sigma/m_a$ and $-p_b\cdot\sigma/m_b$ for the ortho-quark and para-quark propagators, and converts a zero-entropy M function to the associated S matrix by means of the universal connection (for each quark line)

$$S(p_a,p_b)=\sqrt{v_a\cdot\tilde{\sigma}}M(p_a,p_b)\sqrt{v_b\cdot\tilde{\sigma}}\ , \tag{27}$$

then the value of $S(p_a,p_b)$ corresponding to the ortho-quark (para-quark) part of the quark propagator in $M(p_a,p_b)$ is the lower-right-hand (upper-left-hand) submatrix of the four-by-four matrix designated here:

$$\bar{U}(v_a)U(v_b) \text{ for final}\leftarrow\text{initial}, \tag{28a}$$

$$-\bar{U}(v_a)V(v_b) \text{ for final}\leftarrow\text{final}, \tag{28b}$$

$$-\bar{V}(v_a)U(v_b) \text{ for initial}\leftarrow\text{initial}, \tag{28c}$$

or

$$\bar{V}(v_a)V(v_b) \text{ for initial}\leftarrow\text{final}. \tag{28d}$$

Here $U(v)$ and $V(v)$ are the four-by-four matrices obtained from the spinors $U(v,\lambda)$ and $V(v,\lambda)$ defined in (C41) of paper I by omitting the spinor wave functions $\phi_\lambda/\sqrt{2}$ and $\phi^c_\lambda/\sqrt{2}$.[18] In the conditions final←initial, etc., the right-hand designation (here initial) refers to the character of the particle attached to the trailing end of the quark line, and the left-hand designation (here final) refers to the character of the particle attached to leading end of the quark line. As usual, $\bar{U}=U^\dagger\beta$, etc., and $\bar{U}U$, etc., represents a sum over the four-component spinor index.

In (28) no account is taken of statistics—the order of variables is not altered.

If ϕ_λ and ϕ_p are normalized two-component wave functions [as in (C41) of paper I], then in the matrix elements of $S(p_a,p_b)$ the sum of the ortho-graph and para-graph contributions associated with the quark line in question is

$$\langle\phi_\lambda|S(p_a,p_b)|\phi_\rho\rangle=\bar{U}'(v_a,\lambda)U'(v_b,\rho)\cdot F \text{ for final}\leftarrow\text{initial}, \tag{29a}$$

$$\langle\phi_\lambda|S(p_a,p_b)|\phi^c_\rho\rangle=\bar{U}'(v_a,\lambda)V'(v_b,\rho)\cdot F \text{ for final}\leftarrow\text{final}, \tag{29b}$$

$$\langle\phi^c_\lambda|S(p_a,p_b)|\phi_\rho\rangle=\bar{V}'(v_a,\lambda)U'(v_b,\rho)\cdot F \text{ for initial}\leftarrow\text{initial}, \tag{29c}$$

$$\langle\phi^c_\lambda|S(p_a,p_b)|\phi^c_\rho\rangle=\bar{V}'(v_a,\lambda)V'(v_b,\rho)\cdot F \text{ for initial}\leftarrow\text{final}, \tag{29d}$$

where

$$U'(v)=\sqrt{2}U(v), \tag{30a}$$

$$V'(v)=-\sqrt{2}V(v), \tag{30b}$$

and F represents the product of factors associated with the other quark lines, and also the remaining scalar factor f.

When one takes the product of two M functions, with the intermediate metric factor $v\cdot\tilde{\sigma}$ from (8), the corresponding S matrix is

$$\sqrt{v_a\cdot\tilde{\sigma}}M(p_a,-p_b)v_b\cdot\tilde{\sigma}M(p_b,p_c)\sqrt{v_c\cdot\tilde{\sigma}}=S(p_a,-p_b)S(p_b,p_c). \tag{31}$$

Substitution of (29) into (31) yields the intermediate-state factor

$$\sum_{\lambda=1}^{2}U'(v_b,\lambda)\bar{U}'(v_b,\lambda)=1+v_b\cdot\gamma=(\not{p}_p+m_b)/m_b \quad \text{for } p_b^0>0 \tag{32a}$$

or

$$\sum_{\lambda=1}^{2}V'(v_b,\lambda)\bar{V}'(v_b,\lambda)=-1+v_b\cdot\gamma=-(\not{p}_b+m_b)/m_b \quad \text{for } p_b^0<0. \tag{32b}$$

Here use is made of the fact that $p_b=v_bm_b$ ($p_b=-v_bm_b$) if the particle connected to the leading end of the quark line in $M(p_b,p_c)$ is final (initial). Thus, apart from a sign, the familiar Feynman projection operator appears, multiplied, however, by 2. And, correspondingly, the states $\bar{U}'(v_a)\ldots$, etc., that are associated with the external lines of the graph are normalized to 2, rather than 1:

$$\bar{U}'(v,\lambda)U'(v,\lambda)=2=-\bar{V}'(v,\lambda)V'(v,\lambda). \tag{33}$$

These unusual normalization factors have arisen from the fact that the intermediate quark line is carrying four topologically distinct contributions. Since the extra factor of 2 appears in the normalizations of both the spinor wave functions and the propagator one could remove it by a renormalization of the magnitude of the zero-entropy function. However, any such renormalization would upset the fact that the *same* scalar factor f appears in the zero-entropy function for all three types of particles: mesons, baryons, and baryonium. This important "super-symmetry" property arises from the fact that the algebraic factor $F^G(A)$ drops completely out of all zero-entropy discontinuity equations, and leaves the equations that define f independent of particle type.

The question of signs is now discussed. Each zero-entropy function $Z^G(A)$ is a product of an algebraic factor $F^G(A)$, a scalar factor $f^G(A)$, and a statistics sign factor $\sigma^G(A)$. The algebraic factor is the product of the ortho-propagators or para-propagators $p_a\cdot\sigma/m_a$ or $-p_b\cdot\sigma/m_b$ associated with the quark lines of G. The scalar factor $f^G(A)$ is a function of the scalar invariants. The sign $\sigma^G(A)$ was specified at the end of Sec. II.

The sign $\sigma^G(A)$ can also be expressed as $(-1)^\chi$, where χ is the number of permutations needed to take the end points of the directed quark lines of $G(A)$ into an order in which the two end points of each quark line are adjacent, with the leading end point of each such line standing immediately to the left of its trailing end point. The original order of these end points in the graph

$$G(A)=G(A_1,\ldots,A_n)$$

is specified by the order of the corresponding sets of variables A_i, as specified in Sec. II. These rules, together with the rule that the link between A_1 and A_n placed along the top of the graph, give a natural way of ordering the end points of the quark lines of any zero-entropy graph. The statistical factor $(-1)^\chi$ is then plus one or minus one according to whether the connection along the top (i.e., between A_1 and A_n) is a diquark line (i.e., a pair of quark lines) or a solitary quark line. This sign agrees with the one given at the end of Sec. II.

Note that this sign as determined by the rule given in Sec. II is fixed by the character of the *particles* associated with vertices 1 and n: the expression $(-1)^\chi$ in terms of quark lines is merely auxiliary.

Let G_1 and G_2 be two particle-quark graphs. Let G_1 stand to the left of G_2, and consider the product graph $G_1\times G_2$ obtained by joining via sets s_i, certain final-particle vertices of G_2 to corresponding initial-particle vertices of G_1. Each connecting quark line runs either forward (right to left) or backward (left to right).

Let $F^{G_1}\times F^{G_2}$ be the algebraic function obtained by taking the inner product of F^{G_1} and F^{G_2} with respect to the variables associated with the intermediate quark lines of $G_1\times G_2$, including, as in (6), the appropriate metric factor $v\cdot\tilde{\sigma}$ for each such intermediate quark line.

In the simple planar products that occur at the zero-entropy level the function corresponding to product graph $G_1\times G_2$ is

$$F^{G_1\times G_2}=\sigma^{G_1}\sigma^{G_2}F^{G_1}\times F^{G_2}\ . \tag{34}$$

In the general case the ordering of the intermediate variables must be considered, and the function is, according to (6),

$$F^{G_1\times G_2}=(-1)^f\sigma^{G_1}\sigma^{G_2}F^{G_1}\times F^{G_2}\ , \tag{35}$$

where f is the number of permutations of fermion variables needed to bring the two ends of each intermediate fermion line into coincidence.

Let b be the number of backward-directed intermediate quark lines connecting G_2 to G_1. Let $[G_1\times G_2]$ (note the brackets) be the graph obtained by eliminating the vertices on the two ends of each intermediate line of $G_1\times G_2$, continuing the particle and quark lines of G_2 into those of G_1 via the intermediate lines of $G_1\times G_2$ (with no color switching), and then discarding any closed quark loops (i.e., windows). Then

$$\sigma^{[G_1\times G_2]}=\sigma^{G_1}\sigma^{G_2}(-1)^b(-1)^w(-1)^f\ , \tag{36}$$

where $(-1)^w$ is the number of windows. Thus (35) can be written in the alternative form

$$F^{G_1\times G_2}=\sigma^{[G_1\times G_2]}F^{G_1}\times F^{G_2}(-1)^{b+w}\ . \tag{35'}$$

Combining the factor $(-1)^b$ from (35') with (29) one obtains for each intermediate quark line a factor

$$\sum_{\lambda=1}^{2}U'(v,\lambda)\bar{U}'(v,\lambda)\theta(p^0)-\sum_{\lambda=1}^{2}V'(v,\lambda)\bar{V}'(v,\lambda)\theta(-p^0)=(\not{p}+m)/m\ . \tag{37}$$

This is twice the Feynman expression. The remaining algebraic factors are supplied by associating with each external line a factor $U'(p,\lambda)$, $\bar{U}'(p,\lambda)$, $V'(p,\lambda)$, or $\bar{V}'(p,\lambda)$ according to the initial vs final and particle vs antiparticle character of the particle associated with that line. The remaining factor $(-1)^w$ is the analog of the familiar closed-loop factor occurring in the Feynman rules.

The formulas derived above combine in an apparently self-consistent way the zero-entropy functions that arise at the lowest level of the topological expansion with Feynman-type expressions for all higher-order terms in the topological expansion. Convergence of the individual terms, and perhaps even of the expansion itself, should be helped by the (assumed) dual-Regge asymptotic behavior of the zero-entropy amplitudes that here replace the polynomial interaction terms that arise from the notion of a point interaction.

ACKNOWLEDGMENTS

Much of the stimulation for this work originated in conversations with Geoffery Chew. This work was supported by the Director, Office of Energy Research, Office of High Energy and Nuclear Physics, Division of High Energy Physics of the U.S. Department of Energy under Contract No. DE-AC03-76SF00098.

[1]H. P. Stapp, Lett. Nuovo Cimento 19, 622 (1977); F. J. Capra, Phys. Lett. 68B, 93 (1977).

[2]G. G. Rossi and G. Veneziano, Nucl. Phys. B123, 507 (1976).

[3]K. Konishi, Nucl. Phys. B131, 143 (1977).

[4]G. F. Chew, J. Finkelstein, J. P. Sursock, and G. Weissmann, Nucl. Phys. B136, 493 (1978).

[5]J. P. Sursock, Lawrence Berkeley Laboratory Report No. LBL-7588, 1978 (unpublished).

[6]H. P. Stapp, Nuovo Cimento 46A, 37 (1978).

[7]J. Coster and H. P. Stapp, J. Math. Phys. 10, 371 (1969); 11, 1441 (1970); 11, 2743 (1970); and in *Structural Analysis of Collision Amplitudes,* edited by R. Balian and D. Iagolnitzer (North-Holland, New York, 1976), p. 195.

[8]D. Iagolnitzer, *The S-matrix* (North-Holland, Amsterdam, 1978).

[9]J. Coster and H. P. Stapp, J. Math. Phys. 10, 371 (1969), Appendix A.

[10]N. Isgur and G. Karl, Phys. Rev. D 18, 4187 (1978); 19, 2653 (1979).

[11]G. F. Chew and C. Rosenzweig, Phys. Rep. 41C, 263 (1978).

[12]G. F. Chew, Phys. Rev. Lett. 47, 764 (1981).

[13]G. F. Chew, J. Finkelstein, and M. Levinson, Phys. Rev. Lett. 47, 767 (1981).

[14]H. P. Stapp, Lawrence Berkeley Laboratory Reports No. LBL-10774, and LBL 11770, 1981 (unpublished).

[15]R. Espinosa, Ph.D. thesis, University of California, Berkeley (unpublished).

[16]G. F. Chew and M. Levinson, Lawrence Berkeley Laboratory Report No. LBL-14514, 1982 (unpublished).

[17]G. F. Chew, Lawrence Berkeley Laboratory Report No. LBL-14510, 1982 (unpublished).

[18]The normalization factor $1/\sqrt{2}$ was inadvertently omitted in a preprint version of (C41). Here I take $U(v,\lambda)$ and $V(v,\lambda)$ to have the usual normalizations

$$\bar{U}(v,\lambda)U(v,\lambda)=1=-\bar{V}(v,\lambda)V(v,\lambda)\ .$$